Dalton Transactions

ROYAL SOCIETY OF CHEMISTRY

PAPER

View Article Online
View Journal | View Issue

Cite this: *Dalton Trans.*, 2023, **52**, 13732

$Na_{11}Ta_8P_7O_{43}$: (Ta_8O_{33}) bi-capped triangular prisms connected by PO_4 groups resulting in a phase-matched second harmonic response†

Ziyan Lv [a,b] and Rukang Li *[a,b]

Received 13th July 2023,
Accepted 4th September 2023

DOI: 10.1039/d3dt02207b

rsc.li/dalton

Much effort has been devoted to synthesizing nonlinear optical crystals with efficient second harmonic responses. Herein, a tantalum phosphate crystal $Na_{11}Ta_8P_7O_{43}$ with a moderate second harmonic response was obtained using self-fluxes of NaH_2PO_4 and Na_2HPO_4. $Na_{11}Ta_8P_7O_{43}$ belongs to the *Cc* space group of monoclinic systems with cell parameters of a = 8.5710(2) Å, b = 15.1144(4) Å, c = 28.7712 (7) Å, β = 92.304(2)°, Z = 4. Its structural features were unique (Ta_8O_{33}) bi-capped triangular prisms uniformly oriented with a PO_4 connection in the *ab* plane, which were further joined through additional PO_4 groups in the *c* direction, resulting in moderate nonlinear effects. In addition, this crystal has the characteristics of phase-matchable second harmonic generation, a shorter cutoff edge than the known materials $LiTaO_3$ and $KTiOPO_4$, and high transmittance from the visible to the near infrared band, and may serve as a potential nonlinear optical crystal.

1. Introduction

Nonlinear optical (NLO) crystals can broaden the wavelength range of laser radiation by means of laser frequency doubling, sum frequency generation, difference frequency generation, optical parametric oscillation and so on.[1] During the past decades, NLO crystals with efficient second harmonic generation (SHG) have attracted interest, and great efforts have been made to synthesize NLO crystals aimed at specific applications. Excellent and practical second-order NLO crystals not only must satisfy the non-centrosymmetric symmetry, but also have to satisfy the required properties of large nonlinear optical coefficients, phase-matching, a high laser damage threshold, a wide optical transparency window, high transmittance and stable physicochemical properties; they must also be easy to grow into large-sized transparent crystals and easy to process.[2] Currently, most of the commercially used NLO crystals are inorganic, such as KH_2PO_4 (KDP), $KTiOPO_4$ (KTP), $LiNbO_3$ (LN), β-BaB_2O_4 (BBO), LiB_3O_5 (LBO) and $KBe_2BO_3F_2$ (KBBF).[3–8] However, they all have some shortcomings, *e.g.* KBBF is toxic and difficult to grow, KTP crystals cannot completely cover the entire 3–5 μm mid-infrared region, and $LiNbO_3$ has a low laser damage threshold, and so on. According to prior experiences with titanates ($BaTiO_3$ [9] *vs.* $KTiOPO_4$), one of us proposed that the more isolated the titanium group in the crystal, the shorter the UV transmittance cutoff edge and the higher the laser-induced damage threshold (LIDT). And a new titanate $Rb_4Li_2TiOGe_4O_{12}$ (RLTG)[10] has been successfully synthesized and it does show a shorter UV cutoff edge and higher laser-induced damage threshold than KTP (RLTG: 0.28 μm, 6.8 GW cm^{-2} *vs.* KTP: 0.35 μm, 3.4 GW cm^{-2}).

At the same time, phosphate is also a suitable system for exploring NLO crystals because of its rich structure (including the isolated group $(P_nO_{3n+1})^{(n+2)-}$, ring $(P_nO_{3n})^{n-}$, and chain $(PO_3)_\infty$),[11] low growth temperature and a short UV cutoff edge. However, the anisotropy of the phosphate group is small, as are its birefringence and nonlinear susceptibility. Therefore, the introduction of octahedral-coordinated d^0 transition metal cations with larger distortion and larger anisotropy will help to obtain a non-centrosymmetric crystal with large birefringence and large nonlinear susceptibility (second-order Jahn–Teller effect).[12]

A related scientific research study to explore the octahedral-coordinated d^0 transition metal phosphate system has been in progress. In 2022, two kinds of non-centrosymmetric tantalum

[a]*Beijing Center for Crystal Research and Development, Key Laboratory of Functional Crystals and Laser Technology, Technical Institute of Physics and Chemistry, Chinese Academy of Sciences, Beijing 100190, China*
[b]*Center of Materials Science and Optoelectronics Engineering, University of Chinese Academy of Sciences, Beijing 100049, China.*
E-mail: rkli@mail.ipc.ac.cn

† Electronic supplementary information (ESI) available: TG-DSC; X-ray diffraction patterns; fractional atomic coordinates and equivalent isotropic displacement parameters (Å^2); anisotropic displacement parameters (Å^2); selected bond lengths (Å); and the original calculation results. CCDC \ 2249067. For ESI and crystallographic data in CIF or other electronic format see DOI: **https://doi.org/10.1039/d3dt02207b**

phosphate crystals, $Na_3TaP_2O_9$ [13] and $Na_5Ta_8P_5O_{35}$,[14] were discovered by our group. Both crystals had the characteristics of phase-matchability, a large band gap, a wide transmission range and high transmittance. Here, we report a new tantalum phosphate crystal $Na_{11}Ta_8P_7O_{43}$ (denoted as NTPO), in which eight distorted TaO_6 octahedra are connected into a unique (Ta_8O_{33}) bi-capped triangular prism. (Ta_8O_{33}) units are connected by PO_4 groups, indicating that the Ta^{5+} ions in NTPO are more separated than those in $LiTaO_3$.[15] In this paper, the synthesis, structure, characterization methods and theoretical calculation for NTPO are presented in detail.

2. Experimental section

2.1. Synthesis

The polycrystalline powder of the $Na_{11}Ta_8P_7O_{43}$ crystal was prepared by mixing the chemicals of NaH_2PO_4 (Shanghai Aladdin Biochemical Technology Co., Ltd, 99.0%), Na_2HPO_4 (Shanghai Macklin Biochemical Co., Ltd, 99.99%) and Ta_2O_5 (Shanghai Aladdin Biochemical Technology Co., Ltd, 99.99%) according to a stoichiometric ratio of 3 : 4 : 4. Then, the mixture was ground evenly and loaded into a platinum crucible of diameter 20 mm × 20 mm, which was slowly heated to 200 °C overnight to decompose NaH_2PO_4 and Na_2HPO_4. Finally, the sample was slowly heated to 850 °C and kept at this temperature for about 500 minutes to obtain the $Na_{11}Ta_8P_7O_{43}$ polycrystalline powder, which was ground several times during the process.

Single crystals of $Na_{11}Ta_8P_7O_{43}$ were obtained in an open system by the flux method using self-fluxes NaH_2PO_4 and Na_2HPO_4. The compounds NaH_2PO_4, Na_2HPO_4 and Ta_2O_5 were thoroughly mixed at masses of 2.0 g, 1.8 g and 0.5 g, respectively, and placed into a platinum crucible. Then, the crucible was placed in a programmable electric furnace, heated to 850 °C and kept for 24 hours to melt the content completely. Finally, the crucible was cooled to 600 °C with a cooling rate of 2 °C per hour, and then the furnace was switched off. Some millimeter-sized colorless single crystals were obtained.

2.2. Single crystal structure determination

X-ray diffraction data of a transparent, crack-free single crystal $Na_{11}Ta_8P_7O_{43}$ was gathered at 293(2) K using a Rigaku Synergy diffractometer. Data collection, reduction and cell refinement were all completed using CrysAlisPro software. At the Olex2[16] interface, the crystal structure of $Na_{11}Ta_8P_7O_{43}$ was analyzed using SHELXT-2018[17] (intrinsic phasing method) and refined using SHELXL-2014[18] (full matrix least squares on F^2). No additional symmetry was found in the ADDSYM routine of the PLATON[19] program. Crystal data, structure refinement and specific crystallographic information for $Na_{11}Ta_8P_7O_{43}$ can be found in Table 1 and Tables S1–S3,† respectively.

2.3. Powder X-ray diffraction (PXRD)

The powder X-ray diffraction of the polycrystalline powder $Na_{11}Ta_8P_7O_{43}$ was tested using a Bruker D8 Focus diffractometer. Diffraction data were collected in the 2θ range of 5–75°. The results show that the experimental diffraction pattern of $Na_{11}Ta_8P_7O_{43}$ is in line with the simulated pattern of the solved structure (cif file) (Fig. 1). The Le Bail fitting of the experimental XRD pattern using the FULLPROF program is given in the ESI (Fig. S1†).[20–22]

Table 1 Crystal data and structure refinement of $Na_{11}Ta_8P_7O_{43}$

Formula	$Na_{11}Ta_8P_7O_{43}$
Formula weight	2605.28
Temperature/K	293(2)
Crystal system	Monoclinic
Space group	*Cc*
a/Å	8.5710(2)
b/Å	15.1144(4)
c/Å	28.7712(7)
β/°	92.304(2)
Volume/Å^3	3724.17(16)
Z	4
ρ_{calc}/g cm^{-3}	4.647
μ/mm^{-1}	23.967
F (000)	4616.0
Radiation	MoKα (λ = 0.71073)
Independent reflections	7344 [R_{int} = 0.0356, R_{sigma} = 0.0450]
Goodness-of-fit on F^2	1.025
Final *R* indexes [$I \geqq 2\sigma(I)$]	R_1 = 0.0244, wR_2 = 0.0505
Flack parameter	0.023(8)
Final *R* indexes [all data]	R_1 = 0.0259, wR_2 = 0.0510

2.4. Thermal analysis

Thermogravimetry and differential scanning calorimetry (TG-DSC) were performed with 10 mg of NTPO samples in an Al_2O_3 crucible. Then the sample was heated from 50 °C to 1150 °C at a rate of 10 K min^{-1} and finally cooled at 10 K min^{-1} (NETZSCH STA 449F3).

2.5. Diffuse reflectance and infrared spectra

Using $BaSO_4$ as a reference, the diffuse-reflectance spectra were recorded in the range of 200–2500 nm (Cary 7000 UV-vis-NIR spectrophotometer) and the infrared spectra were recorded in the range of 500–4000 cm^{-1} (Varian Excalibur 3100 spectrometer).

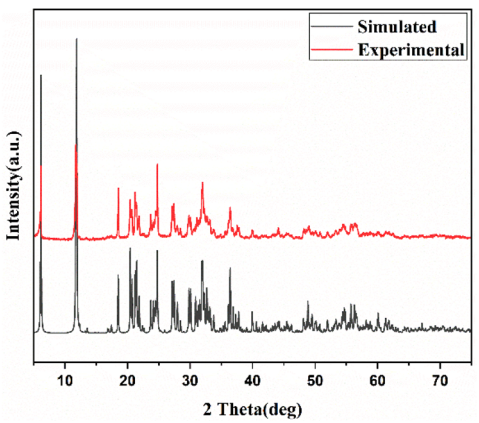

Fig. 1 The simulated and experimental PXRD patterns of $Na_{11}Ta_8P_7O_{43}$.

2.6. SHG tests

The SHGs of $Na_{11}Ta_8P_7O_{43}$ were tested at the wavelength of 1064 nm using a Q-switched Nd:YAG laser adopting the Kurtz–Perry method.[23] The crystalline $Na_{11}Ta_8P_7O_{43}$ powder was ground and sieved into different particle size ranges to compare with the corresponding sizes of KDP (50–100, 100–150, 150–224, 224–300 and 300–355 μm).

2.7. Computational details

Using the CRYSTAL17 code[24] and the B3LYP functional,[25] the electronic band structure of $Na_{11}Ta_8P_7O_{43}$ was computed with a mesh of 6 × 6 × 2 k points in the irreducible reciprocal cell. The pure electronic static optical properties (ω = 0) were calculated with the coupled perturbation Kohn–Sham method.[26–28]

3. Results and discussion

3.1. Structure description

NTPO belongs to the Cc space group of monoclinic systems, and its cell parameters are a = 8.5710(2) Å, b = 15.1144(4) Å, c = 28.7712(7) Å, β = 92.304(2)°, V = 3724.17(16) Å^3 (Table 1). There are 4 chemical formulas within the unit cell of NTPO (Z = 4); all atoms are in the general position. As can be seen from the cell volume, NTPO is a very large structure with the basic structural units of the TaO_6 octahedron and PO_4 tetrahedron. In this structure, all the TaO_6 octahedra are distorted. The eight distorted TaO_6 octahedra form a unique (Ta_8O_{33}) bi-capped triangular prism by sharing O atoms; these interesting structural units were first seen in tantalum phosphate crystals (Fig. 2a). Each (Ta_8O_{33}) unit was connected to six adjacent (Ta_8O_{33}) ones by twelve PO_4 tetrahedra to form an infinite two-dimensional $(Ta_{56}P_{12}O_{243})_\infty$ layer (Fig. 2b). The layers were again joined by isolated PO_4 tetrahedra, forming a three-dimensional network, in which Na^+ ions fill the voids (Fig. 2c). The bond lengths of Na–O, Ta–O and P–O bonds in NTPO were in the range of 2.203(11)–2.959(11) Å, 1.909(10)–2.078(8) Å and 1.485(9)–1.561(9) Å, respectively. The calculated bond valence sums (BVS) of Na, Ta, P and O were 0.8749–1.1868, 4.9348–5.1124, 4.9782–5.0768 and 1.8229–2.2208, respectively, which were in line with their ideal values.

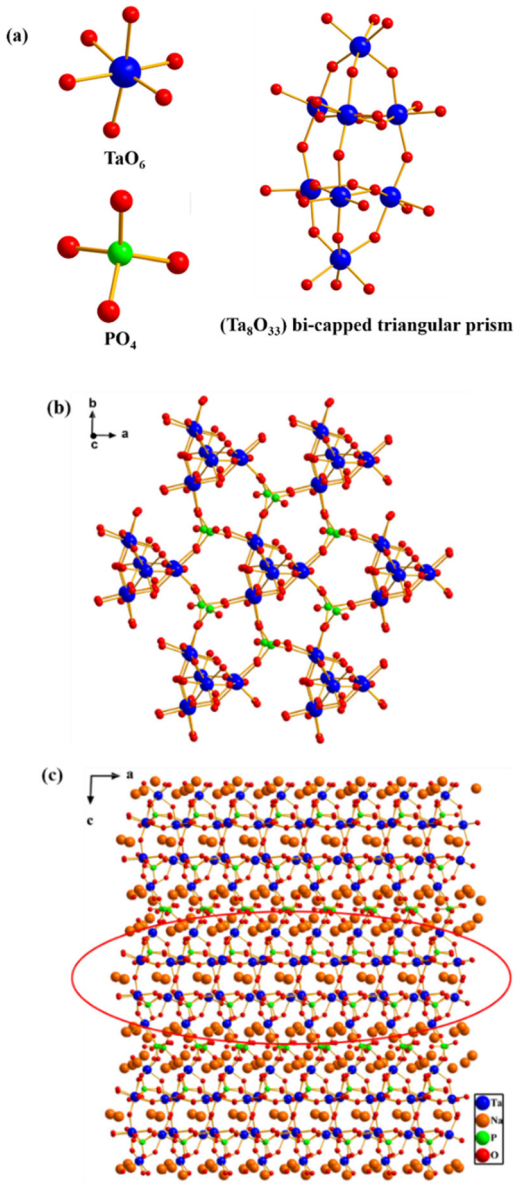

Fig. 2 (a) The structural units, (b) the $(Ta_{56}P_{12}O_{243})_\infty$ plane layer, and (c) the crystal structure of NTPO. Orange – Na, blue – Ta, bright green – P and red – O.

3.2. Thermal analysis

NTPO has no obvious thermal effect in the process of heating and cooling, and its weight decreases significantly from about 900 °C (Fig. S2†). The powder XRD spectra show that NTPO is stable below 850 °C, begins to partially decompose at 900 °C, and completely decomposes into $Na_2Ta_4O_{11}$ at 1350 °C (Fig. S3†).

3.3. Optical properties

The infrared spectrum of the NTPO crystal is shown in Fig. 3(a) and mainly shows the vibrations of the PO_4 group. The absorption observed at the frequencies 997–1190 cm^{-1} and 972 cm^{-1} was attributed to the stretching vibrations of ν_3 and ν_1 of the P–O bonds, respectively. The absorption near the

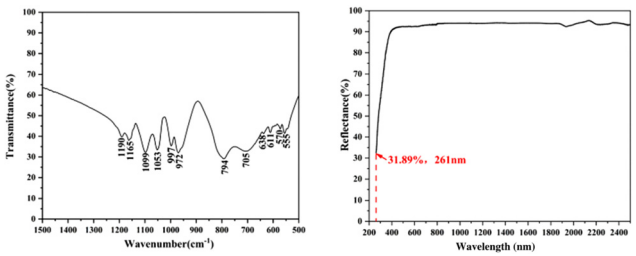

Fig. 3 The infrared spectra (a) and UV-vis-NIR diffuse reflectance spectra (b) of NTPO.

frequency 555–638 cm^{-1} was attributed to the bending vibration of ν_4.[29] And the absorption observed at the frequencies 794 cm^{-1} and 705 cm^{-1} was attributed to the stretching vibrations of ν_{as} and ν_s of the Ta–O bonds, respectively.[30] The UV-vis-NIR spectrum of the NTPO crystal is shown in Fig. 3(b), which has a high transmittance of about 92% in the visible to near-infrared bands. And NTPO still has a reflectance of 31.89% at 261 nm, illustrating that its cutoff edge is less than 261 nm.

3.4. NLO properties

The Kurtz–Perry method was adopted to measure the SHG response of NTPO, which was increased with the increase in particle size. NTPO exhibited a SHG response of about 1× KDP, and was phase-matchable (Fig. 4). On the basis of the anionic group theory,[31] the distorted TaO_6 octahedra and PO_4 tetrahedra were the principal sources of the SHG response of the NTPO crystal. Among them, the distortions of the TaO_6 octahedra were small compared to those in $LiTaO_3$ (0.162 Å),[32] as reflected by bond length differences (Δr) of Ta1–O (0.135 Å), Ta2–O (0.128 Å), Ta3–O (0.053 Å), Ta4–O (0.092 Å), Ta5–O (0.117 Å), Ta6–O (0.128 Å), Ta7–O (0.161 Å), and Ta8–O (0.133 Å), respectively, averaging 0.118 Å. When these distorted TaO_6 octahedra joined to form a (Ta_8O_{33}) unit, the distortions of some of them pointed in opposite directions, therefore cancelling their contributions to the SHG effect. Nevertheless, the (Ta_8O_{33}) unit has an approximate symmetry of D_{3h}, similar to that of the $(B_3O_6)^{3-}$ unit in BBO, and the arrangement of the entire *ab* plane of the crystal is also similar to that of BBO (Fig. S4†). Notably, the SHG response of NTPO is greater than that of the tantalum phosphates discovered by our group previously, such as $Na_3TaP_2O_9$ (0.6× KDP) and $Na_5Ta_8P_5O_{35}$ (0.5× KDP). Moreover, if Ta^{5+} cations are replaced by Nb^{5+} cations, niobium phosphates with the corresponding structures are expected to exhibit a greater NLO–SHG response.[33]

3.5. Theoretical calculations

According to theoretical calculations, NTPO makes an electronic transition from the Γ point (0,0,0) to the C point (1/2,1/2,0) with an indirect band gap of 5.55 eV. The density of states shows that the top of the valence band and the bottom of the conduction band are mainly contributed by the O and Ta orbitals, respectively (Fig. S5†). From the diffuse reflectance spectra, the cutoff edge is less than 261 nm, which is shorter than the cutoff edge of $LiTaO_3$ (280 nm) and KTP (350 nm).[34] Considering Kleinman symmetry,[35] NTPO belongs to the *Cc* space group of the m point group with six independent SHG coefficients (d_{11} = −0.63 pm V^{-1}, d_{12} = 0.78 pm V^{-1}, d_{13} = −0.08 pm V^{-1}, d_{31} = −0.07pm V^{-1}, d_{32} = 0.10 pm V^{-1} and d_{33} = 0.03 pm V^{-1}). Among them, the largest SHG coefficient d_{12} was about twice the KDP coefficient d_{36} and one-third of the BBO coefficient d_{11}, which also indicates that the degree of distortion of the (Ta_8O_{33}) unit is not large enough. In addition, NTPO belongs to the biaxial crystals, with refractive indices of n_x = 1.6839, n_y = 1.6872 and n_z = 1.7444. The relatively large birefringence of Δn = 0.0605 can satisfy the phase matching conditions in the visible range, which is also consistent with our test results. The original results of NTPO are shown in the ESI.†

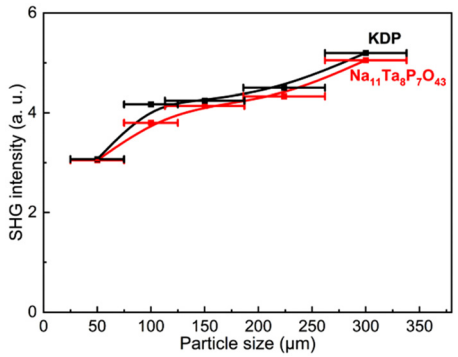

Fig. 4 The SHG curve of NTPO with KDP of different particle sizes as a reference.

4. Conclusion

In summary, a tantalum phosphate $Na_{11}Ta_8P_7O_{43}$ with a phase-matched second harmonic response was synthesized by the flux method. Notably, the second-harmonic response was mainly due to the uniform orientation of the (Ta_8O_{33}) bicapped triangular prisms through PO_4 tetrahedron connections. Simultaneously, this kind of crystal has a shorter cutoff edge than $LiTaO_3$ and KTP and high transmittance from the visible to near infrared bands, and thus may serve as a potential nonlinear optical crystal. And in future work Ta^{5+} ions can be replaced by Nb^{5+} ions to obtain niobium phosphate crystals with a greater NLO–SHG response.

Author contributions

Ziyan Lv: sample preparation, data curation and analysis, and writing – original manuscript. Rukang Li: supervision, funding acquisition, theoretical calculations, data analysis, and review and editing of the manuscript.

Conflicts of interest

There are no conflicts to declare.

Acknowledgements

This work was financially supported by the National Natural Science Foundation of China (52172010).

References

1 V. G. Dmitriev, G. G. Gurzadyan and D. N. Nikogosyan, *Handbook of Nonlinear Optical Crystals*, 1997.

2 W. J. Yao, R. He, X. Y. Wang, Z. S. Lin and C. T. Chen, *Adv. Opt. Mater.*, 2014, **2**, 411–417.
3 J. J. De Yoreo, A. K. Burnham and P. K. Whitman, *Int. Mater. Rev.*, 2002, **47**, 113–152.
4 J. D. Bierlein and H. Vanherzeele, *J. Opt. Soc. Am. B*, 1989, **6**, 622–633.
5 G. D. Boyd, R. C. Miller, K. Nassau, W. L. Bond and A. Savage, *Appl. Phys. Lett.*, 1964, **5**, 234–236.
6 C. T. Chen, B. C. Wu, A. D. Jiang and G. M. You, *Sci. Sin., Ser. B*, 1985, **28**, 235–243.
7 C. T. Chen, Y. C. Wu, A. D. Jiang, B. C. Wu, G. M. You, R. K. Li and S. J. Lin, *J. Opt. Soc. Am. B*, 1989, **6**, 616–621.
8 L. F. Mei, Y. B. Wang, C. T. Chen and B. C. Wu, *J. Appl. Phys.*, 1993, **74**, 7014–7015.
9 S. H. Wemple, M. Didomenico Jr. and I. Camlibel, *J. Phys. Chem. Solids*, 1968, **29**, 1797–1803.
10 M. J. Xia, C. Tang and R. K. Li, *Angew. Chem.*, 2019, **131**, 18425–18428.
11 A. F. Wells, *Structural Inorganic Chemistry*, 1975.
12 E. O. Chi, K. M. Ok, Y. Porter and P. S. Halasyamani, *Chem. Mater.*, 2006, **18**, 2070–2074.
13 Z. Y. Lv and R. K. Li, *Inorg. Chem.*, 2022, **61**, 13554–13560.
14 Q. X. Zhang and R. K. Li, *J. Solid State Chem.*, 2022, **315**, 123544.
15 A. Bruner, D. Eger, M. B. Oron, P. Blau, M. Katz and S. Ruschin, *Opt. Lett.*, 2003, **28**, 194–196.
16 O. V. Dolomanov, L. J. Bourhis, R. J. Gildea, J. A. K. Howard and H. Puschmann, *J. Appl. Crystallogr.*, 2009, **42**, 339–341.
17 G. M. Sheldrick, *Acta Crystallogr., Sect. A: Found. Adv.*, 2015, **71**, 3–8.
18 G. M. Sheldrick, *Acta Crystallogr., Sect. C: Struct. Chem.*, 2015, **71**, 3–8.
19 A. L. Spek, *J. Appl. Crystallogr.*, 2003, **36**, 7–13.
20 A. Le Bail, H. Duroy and J. L. Fourquet, *Mater. Res. Bull.*, 1988, **23**, 447–452.
21 J. Rodríguez-Carvajal, *Phys. B*, 1993, **192**, 55–69.
22 P. Thompson, D. E. Cox and J. B. Hastings, *J. Appl. Crystallogr.*, 1987, **20**, 79–83.
23 S. K. Kurtz and T. T. Perry, *J. Appl. Phys.*, 1968, **39**, 3798–3813.
24 R. Dovesi, F. Pascale, B. Civalleri, K. Doll, N. M. Harrison, I. Bush, P. D'Arco, Y. Noel, M. Rerat, P. Carbonniere, M. Causa, S. Salustro, V. Lacivita, B. Kirtman, A. M. Ferrari, F. S. Gentile, J. Baima, M. Ferrero, R. Demichelis and M. De La Pierre, *J. Chem. Phys.*, 2020, **152**, 204111.
25 A. D. Becke, *J. Chem. Phys.*, 1993, **98**, 5648–5652.
26 M. Ferrero, M. Rerat, R. Orlando and R. Dovesi, *J. Chem. Phys.*, 2008, **128**, 014110.
27 M. Ferrero, M. Rerat, B. Kirtman and R. Dovesi, *J. Chem. Phys.*, 2008, **129**, 244110.
28 M. Ferrero, M. Rerat, R. Orlando and R. Dovesi, *J. Comput. Chem.*, 2008, **29**, 1450–1459.
29 M. V. Sukhanov, E. R. Gobechiya, Y. K. Kabalov and V. I. Pet'kov, *Crystallogr. Rep.*, 2008, **53**, 974–980.
30 A. A. Babaryk, I. V. Odynets, N. S. Slobodyanik, V. N. Baumerb and S. Khainakov, *CrystEngComm*, 2012, **14**, 5071–5077.
31 C. T. Chen, Y. C. Wu and R. K. Li, *Int. Rev. Phys. Chem.*, 1989, **8**, 65–91.
32 R. Hsu, E. N. Maslen, D. Du Boulay and N. Ishizawa, *Acta Crystallogr., Sect. B: Struct. Sci.*, 1997, **53**, 420–428.
33 N. S. P. Bhuvanesh and J. Gopalakrishnan, *J. Mater. Chem.*, 1997, **7**, 2297–2306.
34 A. L. Aleksandrovskii, S. A. Akhmanov, V. A. Dyakov, N. I. Zheludev and V. I. Pryalkin, *Sov. J. Quantum Electron.*, 1985, **15**, 885.
35 D. A. Kleinman, *Phys. Rev.*, 1962, **126**, 1977–1979.